Intelligent Contingencgy Overload-Avoiding Control of BESS for Renewable-Rich Local Area

Gonzalez-Longatt, F.; Astapov, Victor ; Rueda, José Luis; Palensky, Peter; Abdellah, Kouzou; Olivo, Franklin ; Chamorro, Harold R.

DOI
10.1109/SSD54932.2022.9955825

Publication date
2022

Document Version
Final published version

Published in
Proceedings of the 2022 19th International Multi-Conference on Systems, Signals & Devices (SSD)

Intelligent Contingencgy Overload-Avoiding Control of BESS for Renewable-Rich Local Area

F. Gonzalez-Longatt
Department of Electrical Engineering, Information Technology and Cybernetics
University of South-Eastern Norway
Porsgrunn, Norway
fglongatt@fglongatt.org

Victor Astapov
Department of Electrical Engineering and Mechatronics
Tallinn University of Technology
Tallinn, Estonia
vic.astapov@taltech.ee

Jose Luis Rueda and Peter Palensky
Department of Electrical Sustainable Energy
Delft University of Technology
Delft, Netherlands
J.L.RuedaTorres@tudelft.nl
P.Palensky@tudelft.nl

Kouzou Abdellah
Laboratoire d'Automatique appliquee et Diagnostic Industriel (LAAD)
Universite de Djelfa
a.kouzou@univ-djelfa.dz

Franklin Olivo
General Manager
Folivo Power Consulting SRL
Santo Domingo, Dominican Republic
folivo@gmail.com

Harold R. Chamorro
School of Electrical Engineering and Computer Science
KTH, Royal Institute of Technology
Stockholm, Sweden
hr.chamo@ieee.org

***Abstract*—An *N*-1 contingency can negatively affect the reliability and security of electrical power systems. A single transmission line outage can cause overload on the local healthy transmission systems, and actions are required to alleviate the overload. Traditionally the system operator uses two actions depending on the operating local area power balance: load shedding or power plant curtailment; both have consequences. This paper proposes the use of a Battery Energy Storage System (BESS) enabled with an intelligent overload avoiding control. The control is illustrated in a test system, and numerical simulations has demonstrated the suitability of the proposed approach.**

Keywords—Overloading, BESS Control Strategy, Reliability, Transmission System Security, PV Power Plant.

I. Introduction

Clean power generation relies on the use of environmentally friendly generation, technological developments together with appropriate market signals motivate the increased use of this kind of generation of electricity in modern power systems [1]. Weather dependent technologies such as solar photovoltaic (PV) and wind power are emerging as competitive generation technologies in the generation mix of modern power systems [2]. However, weather dependent technologies tend to have intermittent and/or highly variable power production [3].

Electrical Energy Storage Systems (EESS) offer a wide range of technologies that can be used together with the weather-dependent generation or stand-alone to provide many of the most valuable services in modern power systems [4]. In particular, the Battery Energy Storage Systems (BESSs) have quickly transformed into a predilected option [5], [6]. Utility-scale lithium-ion (Li-ion) battery systems are dominating the market, and a recent report [7] indicates that the BESS markets worldwide was US$137/kWh during 2020, a fall of 89% from 2010.

A significant advantage provided by BESS is flexibility in addressing the full range of active and reactive power needs. The use of utility-scale BESS is vastly documented in the scientific literature, and it includes many applications providing a wide range of services as [8]: Arbitrage, reducing renewable energy curtailment, load-levelling, firm capacity or peaking capacity, transmission and distribution upgrade deferrals, black start. The characteristics of the BESSs (e.g., storage system size, target discharge duration, minimum cycles/year, etc.) are intrinsically dependent on the specific application. The transmission and distribution upgrade refers (or avoids such investments entirely) to delaying utility investments in transmission/distribution system upgrades by installing an appropriately sized and located BESS. This application typically uses BESS that ranges from 10–100 MW with a target discharge duration range of 2-8 hours and a minimum of 10-50 cycles/year [9], [10]. The transmission congestion is typically related to transmission facilities no able to transmit the energy from dispatched power plants that cannot be delivered to all or some loads [9], [10]. When the BESS is used for congestion relief, the energy storage system ranges from 10–100 MW with a targe discharge duration that ranges between 1-4 hours and a minimum 10-50 cycles/year [9], [10].

The curtailing of weather-dependent renewable generation is an increasing concern in electric power systems, especially for proprietary PV and wind power plants. The curtailment loses potentially useful energy and may impact Power Purchase Agreements (PPA). Many situations can cause renewable energy curtailment, but always as a measure to ensure the system stability and reliability [11], [12]. One reason for renewable energy curtailment is transmission system constraints, and this situation is even worst considering the *N*-1 contingency.

This paper looks into the use of BESS control to reduce the transmission system (transformer/lie) overloading under an *N*-1 contingency of a rich PV generation area. The proposed BESS control targets to reduce the transmission line overload by internationally charging the BESS to de-load the transmission line at a time that reduces the PV curtailment.

This scientific paper focuses on the thermal limit of the transmission line to limit the temperature attained by the energised conductors and the resulting sag and loss of tensile strength. Other technical limits as surge impedance loading limits and voltage drop can be added as additional constraints to the control without affecting the proposed approach in this paper. Sections II conceptualise the proposed intelligent control, and Section III shows the simulation results that illustrate the suitability of the proposed approach. Finally, section IV concludes.

2022 19th International Multi-Conference on Systems, Signals & Devices (SSD) | 978-1-6654-7108-4/22/$31.00 ©2022 IEEE | DOI: 10.1109/SSD54932.2022.9955825

II. Proposed Intelligent Control

An illustrative test system is shown in Fig. 1. It is a representative reduced equivalent of a large multi-machine power system, where a transmission system interconnects a local area to an external power system. The local area is represented by a lumped load and an equivalent PV Power Plant (PVPP). The transmission system consists of two transmission lines (line-1 and line 2) in parallel connected to two transformers (Trx1 and Trx 2) in a step-up substation.

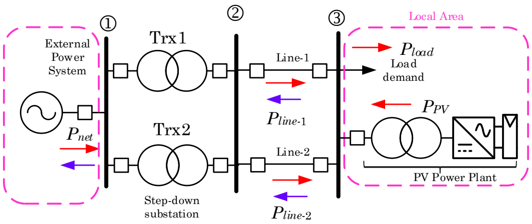

Fig. 1. Test System. Normal operation of the Local Area connected to an external power system through a transmission system.

The massive penetration of high PV generation on power systems affected the active power balancing process, and it has been identified as a challenge in the power system operation. The PV generation has a straightforward pattern (and well known), and when combined with the load demand, the effect on the transmission system loading can be significant, e.g., when solar power production is high, and power demand in the grid is low, power flow can be reversed, voltage might raise/reduce (depending on the reactive power operation mode of the PVPP), active power losses can reduce/increase, etc.

Karen Edson, Vice-President, Policy & Client Services of California Independent System Operator (CAISO), introduced the concept of *duck curve* to describe the effect of the utility-scale PV production patterns in the Californian electricity grid. The duck curve -named after its resemblance to the silhouette of a duck— is a graph of power production over the course of a day that shows the timing imbalance between peak demand and energy production, specifically the photovoltaic. K. Edson introduced the term in 2021, and it is used to explain that in some locations and markets, the maximum production of renewable resources and the peak demand are not coincident. If the installed capacity of solar PV is utility-scale, the amount of power production increases during high insolation hours, but the daily peak demand occurs after sunset, when solar power is no longer available.

The duck curve is always present when the total instantaneous active power production of the PV assets, $P_{PV}(t_i)$ is below the instantaneous values of the total power demand $P_{load}(t_i)$ -see Fig 1. The specific shape of the duck curve also requires a primary peak of the load demand that is outside of the period of PV generation as it defines the neck and head of the duck.

The transmission system exhibits no congestion during the normal operation of the test system as a consequence the power transfer at the transmission lines are inside the limits ($I_{line\text{-}1} < I_{max}$ and $I_{line\text{-}2} < I_{max}$, shown in Fig. 1). However, an N-1 contingency in the radial topology of the transmission system may produce an overload at the healthy transmission line. Consider, the transmission line line-2 is disconnected, therefore the active power flow from/to the local area must flow throw the heathy line (line-1, see Fig 2).

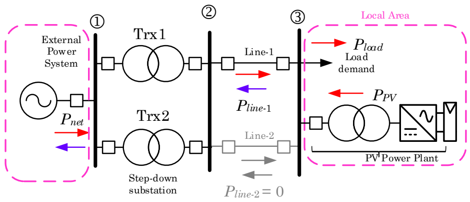

Fig. 2. Test System. *N*-1 contingency operation of the Local Area connected to an external power system. Line-2 outage at line-1 healthy.

The active power flow (considering direction defined by the red arrow) at the healthy transmission line must satisfy the classical power balance principle at any time period ($t_k = 1, \ldots, N_{periods}$)

$$P_{line-1}(t_k) = P_{load}(t_k) - P_{PV}(t_k) \tag{1}$$

The magnitude and direction of $P_{line\text{-}1}(t_k)$ is defined by the magnitudes of the load demand $P_{load}(t_k)$ and the generation of the PVPP $P_{PV}(t_k)$. The overload condition of the transmission line-1 is found at t_k where:

$$\left|P_{line-1}(t_k)\right| = \left|P_{load}(t_k) - P_{PV}(t_k)\right| > P_{line-1,\max} \tag{2}$$

The equation above can be used to define specific moments of the day where the overload condition is present following the line-2 contingency.

Reducing the overload condition can be solved by two practical options: (i) adjusting the load demand or (ii) adjusting the PVPP production. The first involves disconnecting load (shedding) negatively impacting the financial and reliability indicators. The second option is referred to as energy curtail, and it also has financial implications. Both of the previously presented options exhibit a negative effect to one or all parties, as a consequence, an alternative mechanism is needed. As the load demand is stochastically changing over time as the weather-dependent renewable energy production, a flexible solution is attractive.

This scientific paper is innovating by proposing an alternative mechanism to solve the overload of the healthy transmission line during the *N*-1 contingency situation by taking advantage of the flexibility provided by BESS. Consider an appropriately sized BESS is installed in the local area, the active power injection/absorption of the BESS – $P_{BESS}(t_k)$– can be used to control the power flow a the healthy transmission line-1 (see Fig. 3).

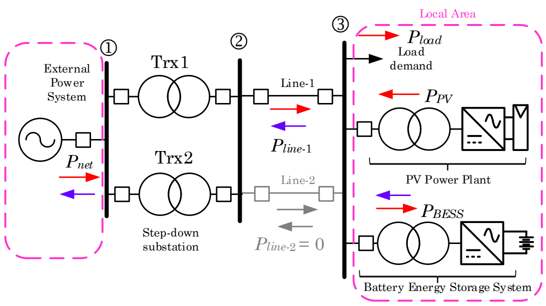

Fig. 3. Test System + Proposed controlled BESS. *N*-1 contingency operation of the Local Area connected to an external power system. Line-2 outage at line-1 healthy.

A specific-case control system is proposed to cope with the problem of overloading the healthy transmission line doing an N-1 contingency situation; the control is named "Intelligent Overload Avoiding Control".

The control system assumes that the BESS is installed in the common point of the transmission lines (bus ③), and measurements are available at the involved transmission lines, PVPP, BESS and the lumped load. The measurements are collected at the field at locally installed voltage, and a current transformer and an industrial computer/controller can obtain the appropriate active power magnitude and directions. The control actions of the proposed controller are taken in the form of active power reference signals (P^*_{BESS}, * is used to identify reference signals), and the signal instructed to charge or discharge de BESS based on the control rules defined below.

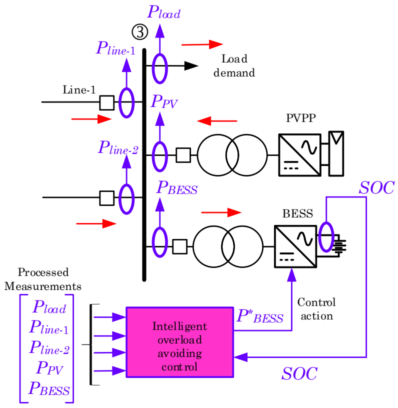

Fig. 4. Illustrative block diagram of the proposed Intelligent overload avoiding control.

A. Condition monitoring

The proposed controller monitors the active power flow of the transmission lines connected to the busbar; if any of the Pline-i (i = 1 and 2, it can be generalised) is zero, the control systems are armed and detect the possibility of an N-1 transmission line contingency. Alternatively, the control can use the binary status of the transmission line circuit breakers to detect the contingency. The controller will attend only contingency at the local transmission system.

The closed-loop control system is also receiving the state-of-change (SOC) signal from the BESS; the intelligent controller can deliver the proposed intelligent overload avoiding action if the SOC of the BESS is inside the operational limits, as a consequence, the controller considers them as:

$$SOC_{\min} \le SOC \le SOC_{\max} \quad (3)$$

where $SOC_{\min}$ and SOC max represent the minimum and maximum state of charge allowed to the battery pack (typically recommended by the manufacturer).

B. Control actions

During an N-1 contingency, the overload of the healthy transmission line can occur in two scenarios.

Local area importing: The active power flow is from the bus ② to ③ ($P_{line\text{-}1}(t_k)>0$), in this case, the active power production of the PVPP is below the load demand ($P_{PV}(t_k)<P_{load}(t_k)$), the overload condition is relief by the intelligently discharging the BESS ($P_{BESS}(t_k)<0$). This control action is taken to avoid load shedding to adjust the loading of the healthy transmission line at t_k. The active power reference of the BESS (P^*_{BESS}) must follow at least:

$$P^*_{BESS}(t_k) > P_{line-1,\max}(t_k) + P_{load}(t_k) - P_{PV}(t_k) \quad (4)$$

Local area exporting: The active power flow is from the bus ③ to ② ($P_{line\text{-}1}(t_k)<0$), in this case, the active power production of the PVPP is larger than the load demand ($P_{PV}(t_k)>P_{load}(t_k)$), the overload condition is relief by the intelligently charging the BESS ($P_{BESS}(t_k)>0$). This control action successfully avoids the PVPP curtailment at t_k. The active power reference of the BESS (P^*_{BESS}) must follow at least:

$$P^*_{BESS}(t_k) < P_{line-1,\max}(t_k) + P_{load}(t_k) - P_{PV}(t_k) \quad (5)$$

III. Simulation and Results

This section is dedicated to illustrating the proposed intelligent overload avoiding control. This section initially shows the simulation scenarios to assess the controller and then show the test system performance without the controller and finally the simulation results of the proposed controller.

A. Scenarios

This subsection describes the two main scenarios considered in this scientific paper. The scenarios are designed to represent the effect of the duck curve where instantaneous the penetration level of PV is used to differentiate the scenarios.

Base Case: No PV generation. The base case considers the test system as shown in Fig. 1, and there is no power production at the PV power plant. Consequently, there is no local generation, and the transmission system must entirely supply the local demand. The local load has two components, a residential equivalent load with a maximum demand of 46.44 MW (@18:57) and a commercial load with a maximum demand of 0.5MW @8:17. When combined, the hourly load profile has a primary peak at eventing and a secondary peak at late morning time, and one small valley Benteen the peak followed by the flat valley during the early hours of the day (see Fig. 5).

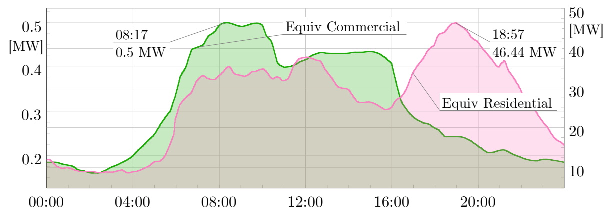

Fig. 5. Base case -*Scenario 0*. Equivalent residential load (pink) and equivalent commercial load (pink).

Scenario 1: Low PV power penetration. The duck-curve is clearly depicted in Fig. 6, the total power demand from the external grid shows a secondary peak of 38.19 MW @ 12:00, but when the PV generation is considered, the total power demand is reduced during the generation period (09:00 to 17:15), the PV generation exhibit a peak of 17.32 MW @ 13:00.

Scenario 2: PV rich area. The effect of the rich-PV area is noticeable when the total instantaneous active power production of the PV assets, $P_{PV}(t_i)$ is larger than the instantaneous values of the total power demand $P_{load}(t_i)$. This situation is depicted in Fig. 7, where there is a clear flow reverse in the active power importation from the external grid. The PV power production peak of 68.88 MW @13:30 causes a reverse in the active power flow from the external grid with a peak of 38.18 MW @ 13:30.

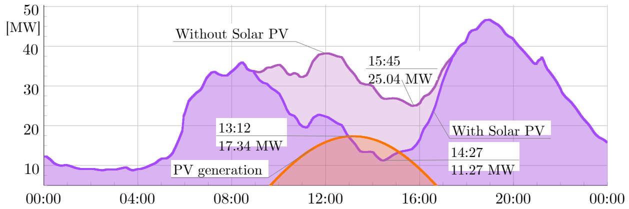

Fig. 6. Active power profiles caused by PV generation: comparison of power flow imported from external (*Scenario 1* and *Base case*, respectively) and details of the PV generation (orange curve)

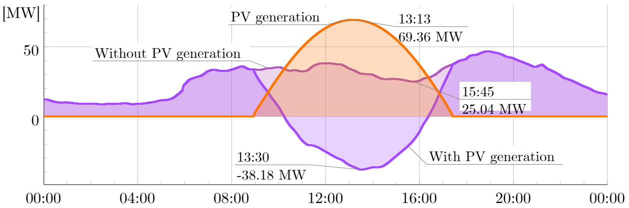

Fig. 7. Active power profiles caused by PV generation: comparison of power flow imported from external (*Scenario 2* and *Base case*, respectively) and details of the rich PV generation (orange curve).

B. *Effect of PV power generation on the transmission line loading*

This subsection explores the effect of the local PV power generation in the loading of the transmission system. In this particular case, the transmission system is simple, and it consists of two identical lines (see Fig. 1). Therefore, the instantaneous loading at any moment is the same for each transmission line ($P_{line\text{-}1} = P_{line\text{-}2}$ (%)). However, the proposed approach in this paper can be extended to more complicated transmission system topologies without losing generality.

During the period of local PV generation, it is well known that the effect of local generation is to reduce the power imported by the transmission line from the external grid (P_{net}). Fig. 8 provide the plots of two situations, considering no PV generation at all ($P_{PV}(t) = 0, \forall t$) and considering low penetration of PV generation. Fig. 8 shows that the local PV generation can reduce the loading of the transmission lines during periods of sunlight (PV generation t∈[09:00,17:15]), the loading of each transmission line is reduced up to 18.29% (14:26).

A further reduction of the transmission lines loading is found when the high PV penetration. A more significant PV power production, like in a PV-rich case, causes a dramatic change in the loading profile of the transmission system; it is clear from Fig. 9 that there are moments where the loading is dramatically reduced to almost 0% at two moments during a day, at 10:15 and 16:45, respectively. What is clear from those results (Fig. 8 and 9), there is no overload at the transmission system even in the PV-rich scenario. However, it must be noticed that the further increase of the PV penetration level can cause a modified loading profile that can produce an increase of the load transmission line loading, e.g., the transmission loading increased up to 61.98% at PV rich scenario, a value that is even higher than the loading when no PV generation is considered.

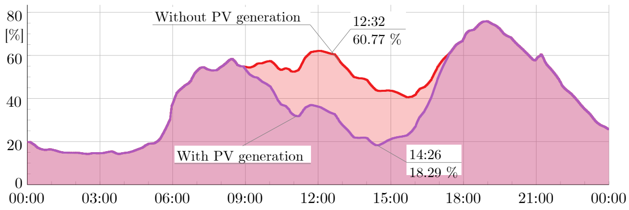

Fig. 8. Transmission line loading: with and without PV generation - *Scenario 1* and *Base case*, respectively.

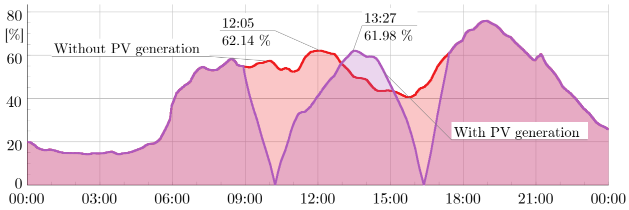

Fig. 9. Transmission line loading: with rich PV-generation and without PV generation -*Scenario 2* and *Base case*, respectivelly).

C. *Effect of a contingency in the transmission line loading*

This subsection explores the effects of a single contingency on the transmission line loading considering the previously studied scenarios (1 and 2). The outage of one transmission line is used as a contingency to assess the loading of the transmission system (healthy transmission line). For simplicity, the transmission line is put out of service at the beginning of the period (00:00), and the loading profile is obtained for the whole day. Fig 10 and 11 show the new loading profiles of Line-1 (%); considering the outage of line-2, a dotted line is used to represent the rated loading of the transmission line, and any value above that line represents an overload. It is clear that the maximum loading peak is caused by the equivalent residential load (~19:00) during evening time where the PV generation cannot contribute to reducing (depicted in Fig. 10 and 11 loading of 151.5% @ 18:52).

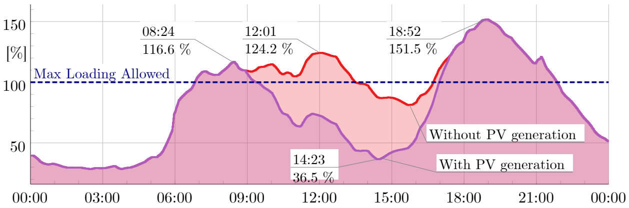

Fig. 10. Transmission line loading (with and without PV generation - *Scenario 1* and Base case, respectivelly) considering the duck-curve scenario and single contingency.

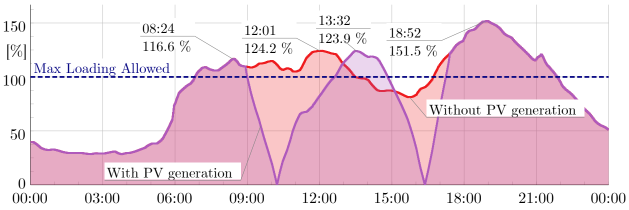

Fig. 11. Transmission line loading (with and without PV generation - *Scenario 2* and Base case, respectively) considering the duck-curve scenario and single contingency)

Scenario 1 and Scenario 2 have positivity reducing the overload at the transmission line. The Line-2 overloading condition is reduced from 9:27 to 16:55 (7h and 28mins) because of the low penetration of the PV generation (Scenario 1). On the other hand, the reduction on the overloading condition is less effective for the case of a rich PV generation (Scenario 2) where the PV generation reduces the overload during two periods (9:00-12:40 and 14:21-17:14) for a total duration of the overload condition (6h and 33min) lower than the Scenario 1. Rich PV generation (Scenario 2) causes a secondary overload in the transmission line when evacuates the maximum PV power generation (between 12:37 and 14:51).

A possible solution to reduce the overload caused by the rich PV penetration case (Scenario 2) is to curtail PV generation. The reduction of the PV generation can reduce the overload but at the same time would cause an economic impact for the proprietary of the PV power plant; as a consequence, this paper is looking into possible options by adding a battery energy storage system that can be used to solve the overloading situation and also enhancing the performance of the system in other (non-contingency) conditions.

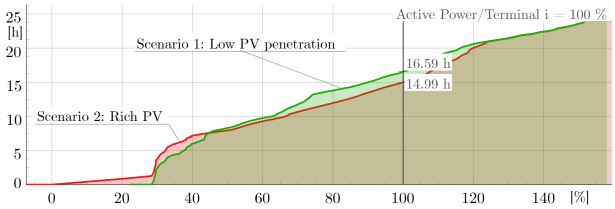

Fig. 12. Duration curve (time [h] versus loading [%]) of the transmission line loading: *Scenario 1* and *Scenario 2*.

Fig. 9 shows the duration curve of the transmission line loading, making clear that the low penetration of PV (Scenario 1) tends to reduce the duration of overloads; the load is below 100% 16.59 hours compared with 14.99 hours reported in rich PV case. However, the reader must recognise that the overload between 17:14 and 21:56 is an overload that can be solved by the PV generation alone as this overload happens after the daylight hours.

D. Use of BESS to alleviate overload during contingency

This section is used to assess the proposed control on its capacity to avoid overloading conditions in the transmission system during a rich PV-generation case (*Scenario 2*). Initially, the suitability of the proposed controller is assessed under normal operation (absence of contingency).

Fig. 13 shows the 24-hour load profile ($P_{line\text{-}1}$ in MW) of one of the transmission lines and the active power injection/absorption of the BESS (P_{BESS} in MW); from the figure is clear that the loading of below the maximum of the transmission line (30 MW = 100%).

Now, the controller is tested under a single contingency condition (line-2 outage). However, depending on the time of the day, the direction and magnitude of the power flow in the healthy transmission lines vary. Fig. 12 shows the highest overloads of the healthy transmission line occurs around 19:00, and a secondary overload peak happens during the maximum PV generation time (~13:00). Those two specific maximum overloading loading periods are used to assess the performance of the proposed intelligent overload avoiding control; the duration of the contingency is assumed to be 2 hours (120 minutes). Fig. 14 and Fig. 15 shows simulation results of the aforementioned contingencies (13:00 and 19:00, respectively), presenting the transmission line power flow ($P_{line\text{-}1}$in MW) and the BESS power (P_{BESS} in MW, negative means charging).

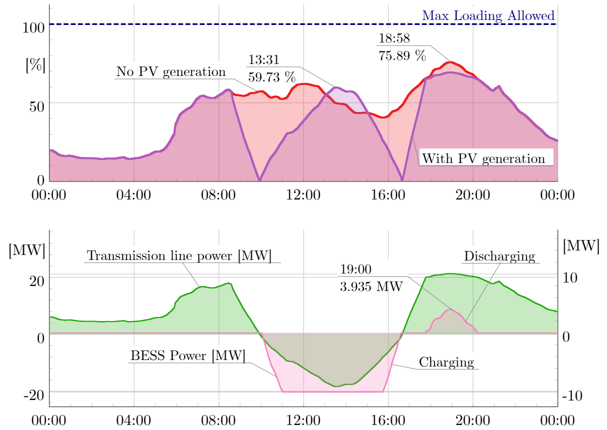

Fig. 13. Normal operation: Line-1 loading (in%, top plot) and Pline-1 and PBESS (in MW, bottom plot). *Scenario 2*.

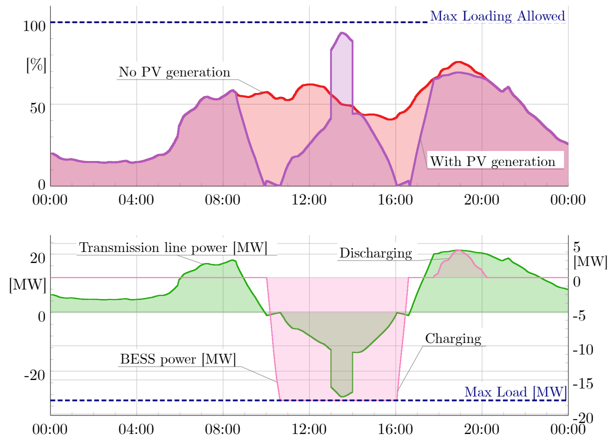

Fig. 14. Single contingency at 13:00: Line-1 loading (in%, top plot) and Pline-1 and PBESS (in MW, bottom plot). *Scenario 2*.

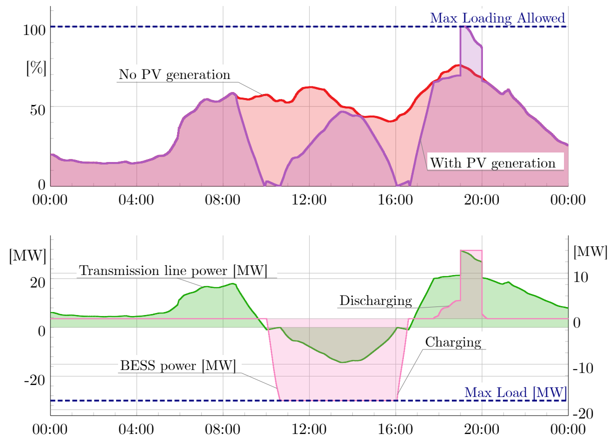

Fig. 15. Single contingency at 19:00: Line-1 loading (in%, top plot) and Pline-1 and PBESS (in MW, bottom plot). *Scenario 2*.

Simulation results of both contingencies scenarios show that the controller is able to quickly reduce the power flow on the healthy transmission line and keep it below the maximum allowed load (30MW). In both cases, the controller takes the opportunity of the PV power production to charge the BESS. Then the contingency occurs at 13:00 (sunlight period); the excess of PV that can cause overload in the transmission line is absorbed by the BESS controlling the line loading. For the case of a transmission line contingency at 19:00, there is no solar PV generation (outside sunlight period) as a consequence; the BESS discharges to compensate the local power demand and keep the transmission loading below its limit.

IV. Conclusions

This paper proposes the use of a Battery Energy Storage System (BESS) as an overloading avoiding control constrained strategy. The strategy is illustrated in a test system with a rich PV installation. The numerical simulations have demonstrated the suitability of the proposed approach on several line loading scenarios monitoring active power.

Acknowledgement

F. Gonzalez-Longatt would like to express his gratitude to DIgSILENT GmbH for all collaborations and for supporting his research.

References

[1] V. Astapov, S. Trashchenkov, F. Gonzalez-Longatt, and D. Topic, "Performance Assessment of TSO–DSO using Volt-Var Control at Smart-Inverters," *Int. J. Electr. Comput. Eng. Syst.*, vol. 13, no. 1, pp. 48–61, Feb. 2022, doi: 10.32985/ijeces.13.1.6.

[2] M. N. Acosta, F. Gonzalez-Longatt, M. A. Andrade, and J. Rueda Torres, "Optimal Reactive Power Control of Smart Inverters: Vestfold and Telemark Regional Network," in *2021 IEEE Madrid PowerTech*, Jun. 2021, pp. 1–6, doi: 10.1109/PowerTech46648.2021.9494911.

[3] B. Mali, A. Shrestha, A. Chapagain, R. Bishwokarma, P. Kumar, and F. Gonzalez-Longatt, "Challenges in the penetration of electric vehicles in developing countries with a focus on Nepal," *Renew. Energy Focus*, vol. 40, no. 1, pp. 1–12, 2022, doi: 10.1016/j.ref.2021.11.003.

[4] F. Gonzalez-Longatt, J. M. Roldan-Fernandez, H. R. Chamorro, S. Arnaltes, and J. L. Rodriguez-Amenedo, "Investigation of Inertia Response and Rate of Change of Frequency in Low Rotational Inertial Scenario of Synchronous Dominated System," *Electronics*, vol. 10, no. 18, p. 2288, Sep. 2021, doi: 10.3390/electronics10182288.

[5] M. N. Acosta, F. Gonzalez-Longatt, M. A. Andrade, J. L. R. Torres, and H. R. Chamorro, "Assessment of Daily Cost of Reactive Power Procurement by Smart Inverters," *Energies*, vol. 14, no. 16, p. 4834, Aug. 2021, doi: 10.3390/en14164834.

[6] F. S. Gorostiza and F. Gonzalez-Longatt, "Deep Reinforcement Learning-Based Controller for SOC Management of Multi-Electrical Energy Storage System," *IEEE Trans. Smart Grid*, vol. 3053, no. c, pp. 1–1, 2020, doi: 10.1109/tsg.2020.2996274.

[7] W. Cole, A. W. Frazier, and C. Augistine, "Cost Projections for Utility-Scale Battery Storage: 2021 Update," *Natl. Renew. Energy Lab.*, no. June, p. 21, 2021, Accessed: Feb. 10, 2022. [Online]. Available: www.nrel.gov/publications.

[8] T. Bowen, I. Chernyakhovskiy, and P. Denholm, "Grid-Scale Battery Storage: Frequently Asked Questions," Accessed: Feb. 10, 2022. [Online]. Available: www.greeningthegrid.org.

[9] D. K. Kim, S. Yoneoka, A. Z. Banatwala, Y.-T. Kim, and K.-Y. Nam, *Handbook on Battery Energy Storage System*, no. December. 2018.

[10] TransGrid, "New South Wales Transmission Annual Planning Report," 2020.

[11] C. Zhang, E. Rakhshani, N. V. Kumar, J. L. Rueda-Torres, P. Palensky, and F. Gonzalez-Longatt, "Real-time Simulation Model of Ultracapacitors for Frequency Stability Support from Wind Generation," in *IECON 2021 – 47th Annual Conference of the IEEE Industrial Electronics Society*, Oct. 2021, vol. 2021-Octob, no. 1, pp. 1–6, doi: 10.1109/IECON48115.2021.9589558.

[12] H. Chamorro, A. Guel-Cortez, E. Kim, F. Gonzalez-Longatt, A. Ortega, and W. Martinez, "Information Length Quantification and Forecasting of Power Systems Kinetic Energy," *IEEE Trans. Power Syst.*, vol. 8950, no. c, pp. 1–1, 2022, doi: 10.1109/TPWRS.2022.3146314.